THE JOURNAL OF PROSTHETIC DENTISTRY

RESEARCH AND EDUCATION

Effect of repeated firing on the topographical, optical, and mechanical properties of fully crystallized lithium silicate-based ceramics

Hanan Al-Johani, BDS, MSD, PGDip,[a] Julfikar Haider, BSc, MA, PhD,[b] Nick Silikas, BSc, MPhil, PhD,[c] and Julian Satterthwaite, BDS, MSc, PhD[d]

ABSTRACT

Statement of problem. The influence of different firing protocols on the topographical, optical, and mechanical properties of fully crystallized computer-aided design and computer-aided manufacturing (CAD-CAM) lithium silicate-based glass-ceramics (LSCs) for dental restorations remains unclear.

Purpose. The purpose of this in vitro study was to investigate the effect of different firing regimens on the surface roughness, gloss, Martens hardness, indentation modulus, biaxial flexural strength, and crystalline structure of fully crystallized CAD-CAM LSCs and the effect of their interposition on the irradiance of a light-polymerization unit.

Material and methods. Three fully crystallized CAD-CAM LSC blocks were evaluated (N=150): lithium disilicate (Initial LiSi Blocks; LS), zirconia-reinforced silicate (Celtra Duo; CD), and lithium aluminum disilicate (CEREC Tessera; CT). Specimens were allocated to 5 subgroups according to their firing protocol. LSC roughness (Sa) was measured with an optical profilometer, and gloss (GU) was detected with a gloss meter. Martens hardness (HM) and indentation modulus (E_{IT}) data were obtained from a hardness testing machine. The irradiance of a light-polymerization unit and transmittance of LSCs were measured with an instrument (Managing Accurate Resin Curing-Light Collector; BlueLight analytics, Inc) subsequent to ceramic interposition. Crystalline phases were analyzed by X-ray diffraction, and biaxial flexural strength (σ) was determined by the ball-on-3-ball method in a universal testing machine followed by Weibull analysis to calculate characteristic strength (σ_0) and Weibull modulus (m). Two-way ANOVA and Tukey HSD post hoc tests (α=.05) were used to analyze the data.

Results. Statistically significant differences were found among different treatment groups based on Sa, GU, HM, and E_{IT} values ($P<.001$). Delivered irradiance was significantly reduced following CT ($P<.01$) and glazed LSC ($P<.005$) interposition. CD displayed highest biaxial flexural strength and reliability after 1 firing cycle (σ=568.2 MPa, m=16.8)

Conclusions. The type of material and firing regimens had a significant effect on the topographical, optical, and mechanical properties of fully crystallized CAD-CAM LSCs. Glazing significantly reduced delivered irradiance, Martens hardness, and biaxial flexural strength. (J Prosthet Dent 2024;131:741.e1-e11)

Computer-aided design and computer-aided manufacturing (CAD-CAM) lithium silicate-based glass-ceramics (LSCs) have become popular in the last decade because of their excellent esthetics and mechanical performance.[1,2] Machinable LSCs are composed of binary quartz and lithium dioxide phases produced by controlled crystallization throughout complex multistage temperature-dependent processes, and LSCs have been classified accordingly as partially or fully crystallized blocks.[3–5] Many derivatives of fully crystallized chairside LSCs blocks are commercially available with differing manufacturer guidelines concerning additional heat treatments.[1] Nonetheless, because of the high machinability and brittleness indices of fully crystallized LSCs,[6] corrective firing may be necessary to

Supported by the Saudi Arabian Cultural Bureau (London, England, United Kingdom).
The authors declare that they have no known competing financial interests or personal relationships that could have appeared to influence the work reported in this manuscript.
[a]PhD student, Division of Dentistry, School of Medical Sciences, University of Manchester, Manchester, England, UK.
[b]Associate Professor, Department of Engineering, Manchester Metropolitan University, Manchester, England, UK.
[c]Full Professor, Division of Dentistry, School of Medical Sciences, University of Manchester, Manchester, England, UK.
[d]Full Professor, Division of Dentistry, School of Medical Sciences, University of Manchester, Manchester, England, UK.

Clinical Implications

Clinicians should consider the number of firing cycles of fully crystallized CAD-CAM LSC restorations cautiously. While surface glazing improved the surface texture of LSCs, it decreased their strength, negatively affecting long-term clinical performance.

eliminate milling-induced defects or subsequent to extensive intraoral occlusal adjustments.[7] Repeated firing of fully crystallized LSCs has been reported to alter color stability,[8–10] translucency,[11,12] opalescence,[11] surface texture,[13,14] microstructure,[4,15] hardness,[4,14] flexural strength,[4,10,11,13,14] Weibull modulus,[10,11] fatigue resistance,[15] fracture toughness,[4,16] and bond strengths to resin cements.[17–20] Glazing is often recommended to optimize esthetics and texture after surface characterization or CAD-CAM machining.[21,22] Autoglazing is achieved by heating ceramic restorations in separate firing cycles to melt the most superficial layer, whereas overglazing consists of applying a thin layer of a low-fusing glass and then firing the ceramic restoration, crystallizing and glazing it in a single step.[21,23,24]

Glaze sprays are offered in nonfluorescent and fluorescent forms; the fluorescent form is preferred to mimic the natural dentition and avoid metameric color mismatch.[25–27] Evidence of the toughening potential of a glaze is inconsistent as, theoretically, the lower coefficient of the thermal expansion of glazes as opposed to that of ceramic substrates should yield strengthening compressive stresses that minimize surface flaws.[28,29] Nonetheless, glazing ceramics has been reported not to affect strength significantly[30] nor be detrimental if lateral cracks emerge from extreme compressive stresses upon cooling of the glaze layer.[31–33] Furthermore, the removal of glaze during intraoral adjustments releases its favorable strengthening stresses and exposes the underlying rough ceramic substrate.[31]

The topography of a ceramic restoration affects its esthetic, biological, and mechanical properties; smoother surfaces appear natural and are less prone to pigmentation, plaque retention, and the wear of opposing substrates.[34–39] Hardness is the ability to resist indenter penetration and can be quantified by visual methods that measure indentation dimensions.[4,21,40] Recently, the Martens hardness test has been used to quantify the indentation resistance of dental ceramics through objective force- or depth-controlled settings.[41–43]

The light attenuation of a light-polymerizing unit depends on the composition, thickness, translucency, and shade of the interposing substrate.[44] Identification and quantification of crystal phases by X-ray diffraction can enhance the understanding the crystalline transformations of ceramics after heat treatments.[45,46] The ball-on-3-ball apparatus enables the measurement of the biaxial flexural strength of rectangular-shaped specimens, and its loading approach creates a stress field of mirror-symmetry and minimal friction, mimicking occlusal forces.[47–50]

Studies on the influence of different firing protocols on the behavior of fully crystallized CAD-CAM LSCs are sparse. This study aimed to determine whether different firing treatments would alter the delivered irradiance, light transmission, surface roughness, gloss, hardness, indentation modulus, biaxial flexural strength, and crystalline structure of fully crystallized CAD-CAM LSCs. The null hypothesis was that different firing regimens would not affect the properties of interest in the same materials and that the same firing regimens would generate similar changes in each property of different materials.

MATERIAL AND METHODS

Three fully crystallized CAD-CAM LSC blocks were investigated in this study (N=150): lithium disilicate, zirconia-reinforced silicate, and lithium aluminum disilicate (Table 1).[3,51] Blocks were sectioned with a precision cutting machine (IsoMet 1000; Buehler) into 12×12×1.5 ±0.05-mm specimens, polished with 400-, 800-, 1000-, and 1200-grit silicon carbide disks (Metaserv 250; Buehler) and cleaned ultrasonically for 10 minute. The specimens were randomly allocated into 5 subgroups by simple computerized randomization (IBM SPSS Statistics, v29.0; IBM Corp) to their assigned treatment protocols (Table 2) per manufacturers' firing schedules (Table 3). In subgroups GF1 and GF2, the glaze spray was held 8 cm away from specimens to apply a uniform glaze layer with adequate thickness (confirmed with digital calipers to be 200 ±10 μm, having a frosty appearance in daylight and displaying fluorescence under UV light).[52] Surface roughness was analyzed with an optical profilometer (Talysurf CLI 1000; Taylor Hobson Precision) equipped with an 400-μm chromatic length aberration and a 0.25-μm cut-off length. Six measurements were obtained per specimen from a scanning area of 2.5×2.5 mm, and average roughness values were computed and reported in terms of the Sa roughness parameter (μm) according to the International Organization for Standardization (ISO) 25178–71:2017 standard,[53] where Sa is the arithmetic mean height deviation within a surface area. Gloss was detected by a gloss meter (IG-331; Horiba) with a 20-degree projection angle as specified by the ISO 2813:2014 standard for high gloss surfaces.[54] The specimens were placed in a custom mold to ensure centered

Table 1. Experimental materials

Classification	Material	Code	Manufacturer	Chemical Composition (wt%)
Lithium disilicate glass-ceramic	Initial LiSi Blocks	LS	GC Corp	81% SiO_2, 8.1% P_2O_5, 5.9% K_2O, 3.8% Al_2O_3, 0.6% CeO_2, 0.5% TiO_2
Zirconia-reinforced lithium silicate glass-ceramic	Celtra Duo	CD	Dentsply Sirona	58% SiO_2, 18.5% Li_2O, 10.1% ZrO_2, 5% P_2O_5, 1.9% Al_2O_3, 2%CeO_2, 1% Tb_4O_7
Lithium aluminum disilicate glass-ceramic	CEREC Tessera	CT	Dentsply Sirona	90% $Li_2Si_2O_5$, 5% Li_3PO_4, 5% $Li_{0.5}Al_{0.5}Si_{2.5}O_6$
Glaze spray	Universal Spray Glaze Fluo	—	Dentsply Sirona	Silicate glass, isopropyl alcohol, isobutane propellant, fluorescing agent.

Table 2. Experimental subgroups

Subgroup	Description
NF	No firing treatment
F1	One crystallization firing cycle
F2	Two crystallization firing cycles
GF1	Coated with glaze spray followed by glaze firing cycle
GF2	Coated with glaze spray followed by glaze firing cycle and coated with glaze spray for second time followed by second glaze firing cycle

positioning and covered with an opaque lid to eliminate external light. Three gloss measurements were made per specimen from a 3×3-mm area, and mean values were calculated and reported in Gloss Units (GU), where GU was the percentage of incident light beam/reflected light beam, ranging from 0 (absolute nonreflective surface) to 100 (absolute refractive surface). The Martens hardness and the indentation modulus were measured with a hardness testing machine (Z2.5; ZwickRoell Ltd) from the following equations:

$$HM = \left[\frac{F}{A_s(h)}\right] \text{and } E_{IT} = (1 - v_s^2)\left[\left(\frac{1}{E_r}\right) - \left(\frac{1 - v_i^2}{E_i}\right)\right],$$

where HM is the Martens hardness (N/mm^2), F is the maximum load (N), $A_s(h)$ is the surface area (mm^2) of the indenter at a distance h from the tip, E_{IT} is the indentation modulus (kN/mm^2), v_s is the Poisson ratio of the ceramic specimens (LS v_s=0.198, CD v_s=0.22, and CT v_s=0.229)[1], v_i is the Poisson ratio of the indenter (v_i=0.07),[55] E_r is the reduced modulus of the indentation contact, and E_i is the modulus of the indenter. Six indentations were made per specimen in a force-controlled setting (10-N load) for a 20-second dwell time, and average HM and E_{IT} values were automatically computed by a software program (TestXpert; Zwick GmbH Co).[56] Delivered irradiance (mW/cm^2) was recorded by a spectrophotometer (Managing Accurate Resin Curing-Light Collector; BlueLight analytics Inc) coupled with an analysis software program and a light-emitting diode light-polymerization unit (Elipar S10; 3M ESPE) during a 20-second light exposure cycle. The light-polymerization unit was fixed to obtain zero distance between its tip and the ceramic specimen, with the ceramic specimen centered on the bottom MARC-LC sensor and treated ceramic surfaces facing the light polymerization unit tip. Subsequently, ceramic specimen transmittance T(%) was measured by the equation: $T = \frac{I_t}{I_0}$, where I_t is the transmitted light beam intensity and I_0 is the incident light beam intensity of the LCU ($1600\ mW/cm^2$).[57]

The crystalline phase composition of 1 specimen per subgroup was identified by X-ray diffraction (X'pert Powder; PANalytical), with Cu-Kα radiation (λ=0.51054 Å, 45 kV, and 40 mA), and diffraction profiles were collected in the range of 10<2θ<140 degrees, with a 0.013-degree step size and scan speed of 89 seconds per step. The Scherrer formula[58] was used to estimate average crystallite sizes from diffraction peak widths pertaining to each crystalline phase by using the equation $D = k\lambda / B\cos\theta$, where, k is a geometrical constant (0.89), λ is the wavelength of the X-ray, B is the full width at half maximum of the diffraction peak, and θ is the diffraction angle.

The biaxial flexural strength of the LSCs was determined by the ball-on-3-ball method in a universal testing machine (Z020; ZwickRoell Ltd) (Fig. 1). The specimens were situated between stainless steel balls of

Table 3. LSC firing schedules

Material	Firing Cycle	Standby Temp. (°C)	Closing Time (min.)	Heating Rate (°C/min.)	Firing Temp. (°C)	Holding Time (min.)	Vacuum (On/Off)	Drying Time (min.)
LS	First crystallization cycle	480	4:00	45	750	1:00	On	2:00
	Second crystallization cycle	450	4:00	45	730	1:00	On	2:00
CD	First crystallization cycle	500	3:30	60	820	1:00	Off	2:00
	Second crystallization cycle	500	3:30	60	770	1:00	Off	2:00
CT	First crystallization cycle	400	3:30	60	760	1:30	Off	0:00
	Second crystallization cycle	400	3:30	60	760	1:30	Off	0:00
LS, CD, CT	Glaze cycle	400	2:00	55	760	2:00	Off	0:00

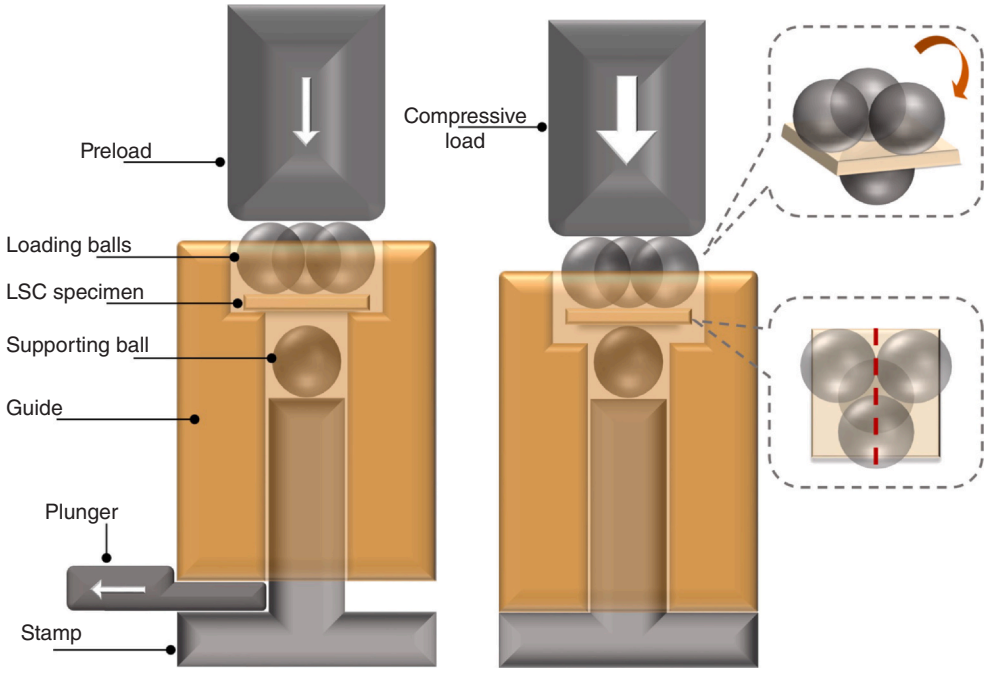

Figure 1. Schematic representation of ball-on-3-ball biaxial flexural strength test; Left: Preload (*small white arrow*) applied via loading cell before plunger removal to ensure simultaneous contact with loading balls. Right: Plunger removed and guide lowered, yielding free rotation of loading balls (*orange arrow*) and stress field with mirror symmetry (*red dashed line*). Upon applying compressive load (*large white arrow*), biaxial flexural strength σ (MPa) computed.

equal radii with 3 loading balls on the tensile side and a support ball on the compressive side, with the surfaces of the treated specimens facing away from the tensile stresses. A 20-kN compressive load cell was used to apply a preload of 10 N and then proceeded at 0.5 mm/minute crosshead speed until specimen fracture. The flexural strength σ (MPa) was determined as the maximum stress created on the specimen's tensile side at fracture and was calculated from the following equation: $\sigma = \delta F_{max}/t^2$, where t is the thickness of the specimen, F_{max} is the force at fracture, and δ is a function derived from finite element analysis[49] based on the radii of the support balls (R_a), specimen thickness (t), and Poisson ratio (v). δ was calculated from the equation:

$$\delta = 0.323308 + \frac{\left[[(1.30843 + 1.44301v)]\left[1.78428 - 3.15347\left(\frac{t}{R_a}\right) + 6.67919\left(\frac{t}{R_a}\right)^2 - 4.62603\left(\frac{t}{R_a}\right)^3\right]\right]}{\left[1 + 1.71955\left(\frac{t}{R_a}\right)\right]}.$$

The Weibull analysis was performed to assess reliability in the flexural strength as a result of different heat treatment regimens. The Weibull modulus (m) was calculated from the equation:

$$P_f(\sigma) = 1 - \exp\left[-\left(\frac{\sigma}{\sigma_0}\right)^m\right],$$

where P_f (σ) is the failure probability for a given flexural strength, σ is the fracture strength, σ_0 is the characteristic strength at 63.2% fracture probability, and m is the Weibull modulus.[59] Upper and lower limits of the 95% confidence intervals for σ_0 and m were calculated following DIN ENV 843–5:2007.[60] Sample sizes for roughness, gloss, hardness, indentation modulus, irradiance, and transmission properties were obtained from a power analysis software program (G*power, V. 3.1.3; Heinrich Heine University Düsseldorf). An eta-squared value of 0.06 was used to estimate effect sizes that yielded 80% power.[61] Sample size for flexural strength testing was chosen from the ISO 6872:2015 standard.[62] Data normality and homogeneity assumptions were confirmed by the Kolmogorov-Smirnov test and Levene test (α=.05). Two-way ANOVA was applied to evaluate the effects of ceramic material, firing treatment, and their interaction (α=.05), and the Tukey HSD post hoc test was used for pair-wise comparisons (α=.05). A statistical software program (IBM SPSS Statistics, v29.0; IBM Corp) was used for all statistical analyses.

RESULTS

The ANOVA table for all analyses is presented in Table 4. The 2-way ANOVA indicated a significant effect of material, firing treatments, and their interaction on mean Sa and GU values ($P<.001$) (Fig. 2A, B), and a negative correlation was found between roughness and gloss ($r=-0.715$, $P<.001$). Furthermore, ANOVA detected a significant effect of variables on the delivered irradiance ($P<.001$) (Fig. 2C) and T of LSCs ($P<.05$) (Fig. 2D). LS and CT specimens coated with 2 glaze layers exhibited significantly lower delivered irradiance

Table 4. ANOVA table for surface roughness, gloss, Martens hardness, indentation modulus, delivered irradiance, light transmission, and biaxial flexural strength df, degrees of freedom

Parameter	Effect	Sum of Squares	df	Mean Square	F	*P*
Roughness	Material	.019	2	.010	126.801	<.001
	Treatment	.233	4	.058	758.510	<.001
	Material × Treatment	.008	8	.001	13.116	<.001
Gloss	Material	1391.876	2	695.938	80.180	<.001
	Treatment	6879.388	4	1719.847	198.145	<.001
	Material × Treatment	648.112	8	81.014	9.334	<.001
Martens hardness	Material	1503973.474	2	751986.737	55.270	<.001
	Treatment	7045782.376	4	1761445.594	129.463	<.001
	Material × Treatment	3270874.838	8	408859.355	30.050	<.001
Indentation modulus	Material	481.208	2	240.604	22.445	<.001
	Treatment	3324.377	4	831.094	77.531	<.001
	Material × Treatment	1679.335	8	209.917	19.583	<.001
Delivered irradiance	Material	1072574.747	2	536287.373	3758.321	<.001
	Treatment	24789.867	4	6197.467	43.432	<.001
	Material × Treatment	3896.453	8	487.057	3.413	.003
Light transmission	Material	29.240	2	14.620	1.084	.035
	Treatment	53.933	4	13.483	1.000	.015
	Material × Treatment	108.154	8	13.519	1.002	.054
Biaxial flexural strength	Material	394237.548	2	197118.774	94.109	<.001
	Treatment	337217.135	4	84304.284	40.249	<.001
	Material × Treatment	93593.542	8	11699.193	5.585	<.001

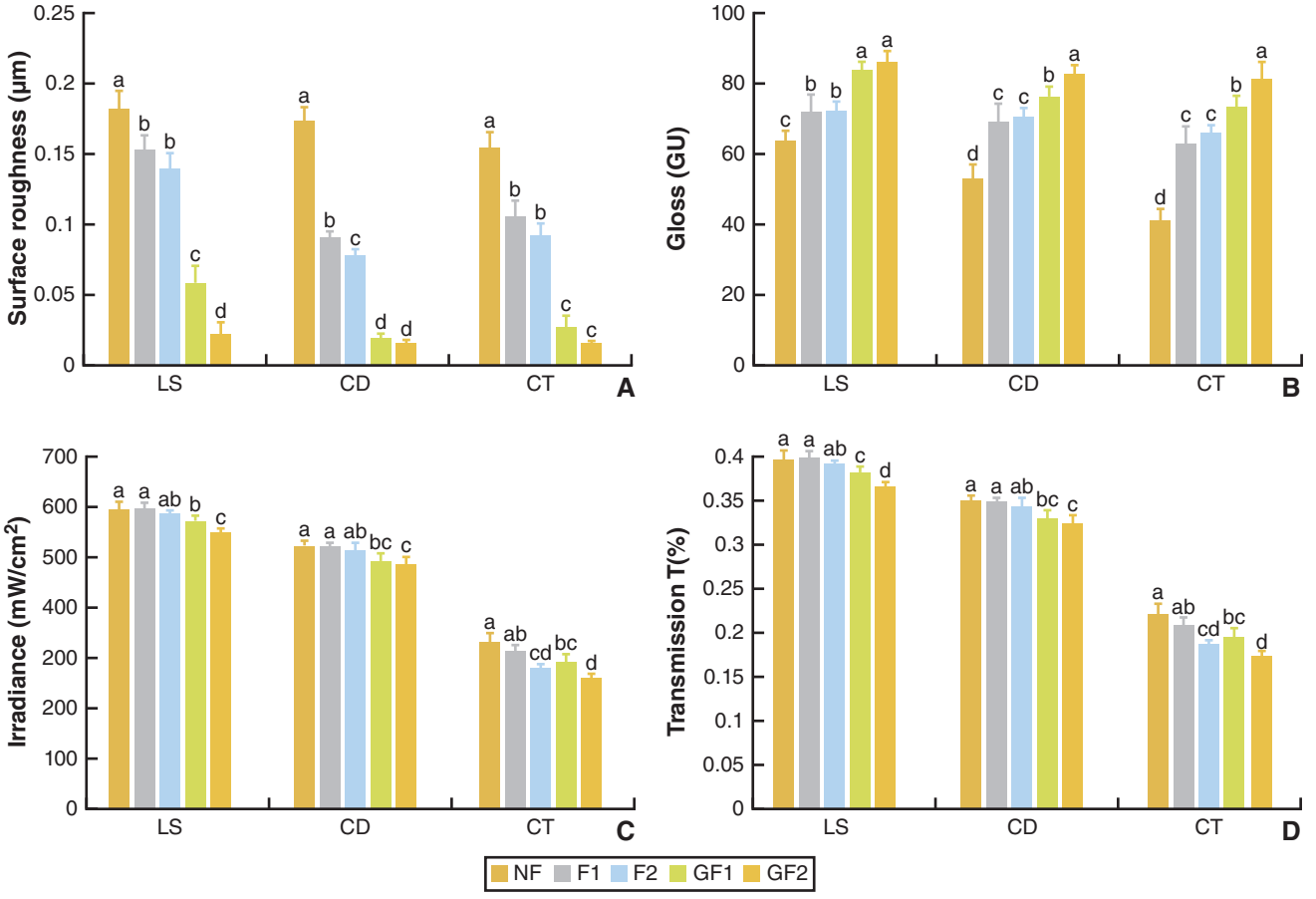

Figure 2. Measurements of fully crystallized computer-aided design and computer-aided manufacturing lithium silicate-based glass-ceramic surfaces after heat treatment. A, Surface roughness Sa (μm). B, Gloss (GU) measurements. C, Mean delivered irradiance (mW/cm^2). D, Transmission T(%) Different letters indicate significant statistical differences between heat treatments within same material ($P \leq .05$).

Table 5. Martens hardness (N/mm^2) and indentation modulus (kN/mm^2) of fully crystallized computer-aided design and computer-aided manufacturing lithium silicate-based glass-ceramics after heat treatment

Group	Martens Hardness (N/mm^2) Mean ±Standard Deviation	Indentation Modulus (kN/mm^2) Mean ±Standard Deviation
LS - NF	4425.1 ± 111.9^{a1}	82.2 ± 3.9^{a1}
LS – F1	4312.0 ± 121.3^{a1}	80.3 ± 4.5^{a1}
LS - F2	3693.6 ± 235.4^{b12}	67.8 ± 5.9^{b2}
LS – GF1	3601.0 ± 86.2^{b1}	68.3 ± 2.7^{b1}
LS - GF2	3239.5 ± 101.8^{c1}	59.2 ± 4.2^{c1}
CD - NF	3255.3 ± 176.3^{c3}	63.5 ± 1.6^{b3}
CD – F1	4125.0 ± 125.7^{a2}	81.8 ± 2.8^{a1}
CD - F2	3870.9 ± 100.1^{b1}	77.1 ± 3.9^{a1}
CD – GF1	3384.3 ± 67.5^{c2}	64.3 ± 1.9^{b2}
CD - GF2	3294.5 ± 46.9^{c1}	57.9 ± 1.2^{c1}
CT - NF	3886.3 ± 86.9^{a2}	73.8 ± 5.3^{a2}
CT – F1	3835.0 ± 87.8^{a3}	70.4 ± 2.9^{ab2}
CT – F2	3426.5 ± 106.6^{b2}	66.2 ± 2.2^{bc2}
CT – GF1	3432.0 ± 50.6^{b2}	61.9 ± 1.1^{c3}
CT – GF2	3068.5 ± 113.4^{c2}	54.5 ± 1.4^{d1}

Different superscript letters indicate significant statistical differences between heat treatments within same material $P \leq .05$).

Different superscript digits indicate significant statistical differences between materials within same heat treatment ($P \leq .05$).

and T. Material type, firing treatments, and their interaction significantly altered HM and E_{IT} ($P<.001$) (Table 5). HM of CD increased after the first firing cycle, whereas LS and CT were harder in nonfired states. The crystalline phase X-ray diffraction (XRD) graphs of LSCs are given in Figure 3, and the crystal sizes in Table 6. The 2-way ANOVA showed a significant effect of all variables and their interaction on σ ($P<.001$) (Fig. 4). Table 7 presents the σ_0, m, and R^2 obtained from plotting the LSC strength values. Figure 5 illustrates Weibull probability plots confirming that the dispersion of strength data fitted within the model ($0.841<R^2<0.974$). The σ_0 was highest in CD after 1 firing cycle (σ_0=812.4 MPa) and lowest in CT after 2 glaze cycles (σ_0=317.3 MPa).

DISCUSSION

This in vitro study investigated the effects of different firing regimens on the topographical, optical, and mechanical properties of fully crystallized CAD-CAM LSCs. The null hypotheses that different firing regimens would not affect the properties of interest in the same materials and that the same firing regimens would generate similar changes for each property in different materials were rejected because different firing regimens, regardless of the evaluated material, displayed different results in the tested properties and different materials, regardless of the firing regimen, also exhibited different results in the evaluated properties.

Roughness and gloss are inversely related parameters frequently used to describe the surface of ceramics after heat treatment.[39] Ceramic roughness above 0.2 μm has been associated with increased bacterial retention, appearance perception, and antagonistic wear.[34–36] In their unfired condition, LSCs exhibited minimally different Sa values (0.15 to 0.18 μm), which could be justified by compositional differences (Table 1), crystalline size (Table 6), and density (LS=55 vol%, CD=51 vol%, and CT=47 vol%).[1,3,63] A second firing further decreased Sa, consistent with previous studies,[9,14,64,65] and was rationalized by the crystal size fluctuations depending on repeated heat treatments (Table 6). Moreover, the LSCs became smoothest after glazing as a function of the homogenous unfilled glass coating.[22,37,66] The GU of dental materials should range between 40 and 60 to mimic that of enamel (40 to 52 GU).[37,38] In the present study, the gloss meter incident light angle was fixed at 20 degrees[52] and so gloss was mainly related to the LSC surface topography and refractive index. Firing treatment increased GU (Fig. 2B), which is explained by the corresponding changes of the LSC crystal sizes altering their light reflection. Nonetheless, all the LSCs displayed satisfactory gloss (GU>40), regardless of their firing condition. The minimum irradiance of an LCU needed for camphorquinone-based resin cement polymerization is 800 mW/cm^2 within 20 seconds[38] Significant reduction in the delivered irradiance of the LSCs was attributed to the glaze coating (Fig. 2C) and to the CT materials, which could be justified by the presence of virgilite ($Li_{0.5}Al_{0.5}Si_{2.5}O_6$) in CT (Table 1) associated with increased light absorption.[3] Thus, prolonged polymerization times are recommended when cementing LSCs with light-polymerized resin cements because of the considerable irradiance decline below the required threshold (< 800 mW/cm^2)in all treatment groups.[38] Hardness is a significant nondestructive durability parameter[38] that can predict the wear performance of LSCs. The Martens hardness test detects indentation resistance simultaneously during an indenter's loading and unloading process, overcoming the subjective bias of traditional optical indentation methods.[41] HM signifies the abrasion resistance of a ceramic while E_{IT} quantifies its elastic response upon unloading the indenter and determines degrees of quasi-plastic deformation in its atomic structures.[42] In the present study, irrespective of treatments, LSCs displayed HM>3000 MPa and E_{IT}>50 kN/mm^2 (Table 5), consistent with previous findings.[42,43] HM differed among LSCs after the first firing cycle; however, a similar pattern decline was found after the second firing cycle and after glazing. The correlation between the number of firing cycles and the hardness of ceramics has been reported previously[4,14,46,64,67] and is explained by changes in crystal density and orientation which alter penetration resistance.

XRD analysis of LSCs provides accurate information regarding crystal size, composition, and phase that can

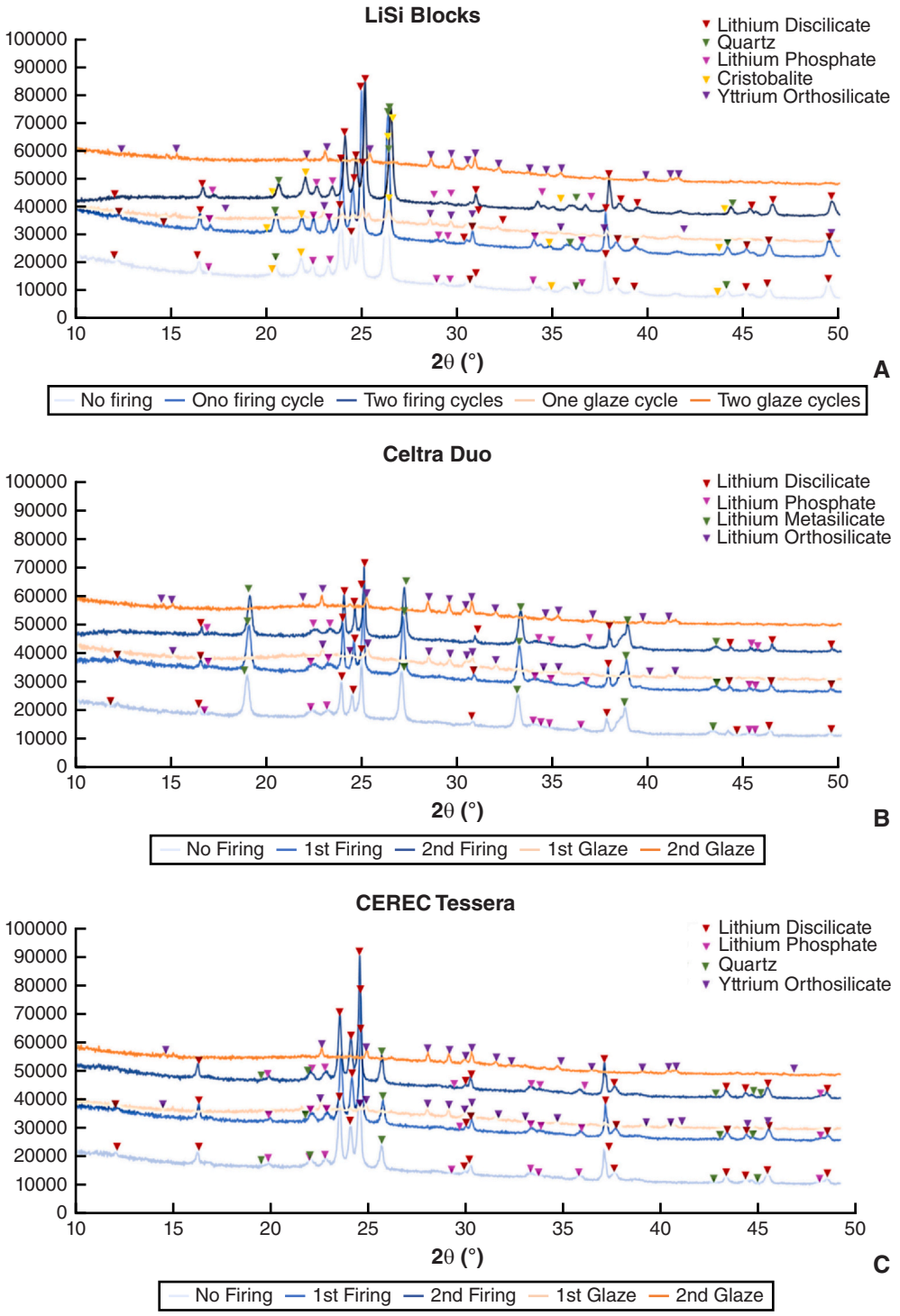

Figure 3. X-ray diffraction patterns obtained for fully crystallized computer-aided design and computer-aided manufacturing lithium silicate-based glass-ceramics after heat treatment identifying corresponding phase assignments. A, Initial LiSi Blocks. B, Celtra Duo. C, CEREC Tessera.

be directly correlated with optical and mechanical properties.[4] When exposed to a higher temperature, XRD peaks corresponding to crystal structures tend to narrow, signifying crystal enlargment.[22,64] Unfired LSCs presented similar crystal microstructures after different firing treatments, similar to those reported previously.[4,5,45] Conversely, glazing LSCs revealed yttrium orthosilicate crystals attributed to the amorphous glass overcoat.[68] The lithium disilicate crystals' XRD peak detected an increase in the crystal size in the LS and CD specimens after 1 firing cycle and in CT specimens after 2 firing cycles, which could be because of the

Table 6. Crystal size (nm) at each stage of LSC firing treatment (NF, F1, F2, GF1, and GF2) and crystalline size variations (nm) after heat treatments. Data from XRD peak at 23.9 degrees corresponded to lithium disilicate, data from XRD peak at 22.4 degrees corresponded to lithium phosphate, data from XRD peak at 26.4 degrees corresponded to quartz, and data from XRD peak at 29.5 degrees corresponded to yttrium orthosilicate

LSC	Crystallite	Crystallite Size (nm)					Crystallite Size Variation after F	Crystallite Size Variation after F2	Crystallite Size Variation after GF1	Crystallite Size Variation after GF2
		NF	F1	F2	GF1	GF2				
LS	Lithium Disilicate	64.4	67.4	69.4	70.6	U/D	3	5	6.2	—
	Lithium Phosphate	74.3	69.8	58.3	141.7	U/D	- 4.5	- 16	67.4	—
	Quartz	52.3	52.6	54.0	46.9	U/D	0.3	1.7	-5.4	—
	Yttrium Orthosilicate	N/A	N/A	N/A	112.9	142.1	—	—	—	29.2
CD	Lithium Disilicate	137.7	140.0	133.7	U/D	U/D	2.3	-4.0	—	—
	Lithium Phosphate	22.2	20.7	27.5	U/D	U/D	- 1.5	5.3	—	—
	Quartz	53.4	56.7	56.0	U/D	U/D	3.3	2.6	—	—
	Yttrium Orthosilicate	N/A	N/A	N/A	856	1014	—	—	—	15.8
CT	Lithium Disilicate	75.2	71.2	79.6	U/D	U/D	- 4.0	4.4	—	—
	Lithium Phosphate	33.9	27.6	30.8	U/D	U/D	- 6.3	- 3.1	—	—
	Quartz	59.1	63.7	69.7	U/D	U/D	4.6	10.6	—	—
	Yttrium Orthosilicate	N/A	N/A	N/A	104.0	149.4	—	—	—	45.4

LSC, lithium silicate-based glass-ceramic; N/A, not available; U/D, undetected; XRD, X-ray diffraction.

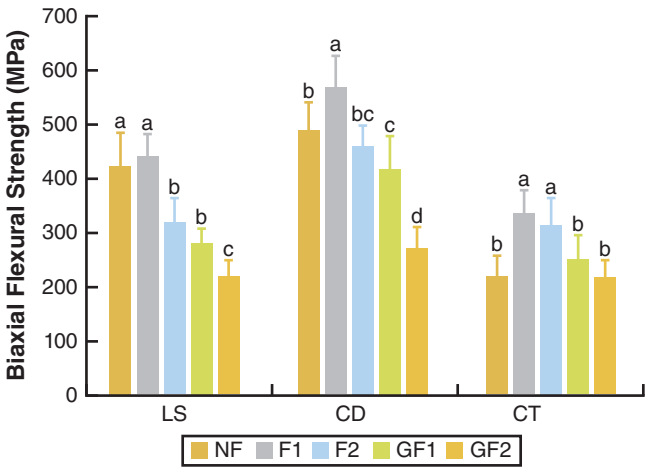

Figure 4. Mean biaxial flexural strength σ (MPa) of fully crystallized computer-aided design and computer-aided manufacturing lithium silicate-based glass-ceramics after heat treatment. Different letters indicate significant statistical differences between heat treatments within same material ($P \leq .05$).

compensation caused by the greater enlargement of quartz crystals in CT materials (Table 6).

The ball-on-3-ball test is an instrumental testing method of measuring the biaxial flexural strength of dental ceramics.[49] The square plate geometry of specimens was chosen based on evidence that verified the comparable flexural strength values of disks and square plates.[49,50] Treated ceramic surfaces faced the compressive loading element to simulate the intraoral environment where polished or glazed surfaces oppose occlusal loads. The minimum σ threshold for monolithic single-unit anterior and posterior restorations is 100 MPa,[62] which was met by all the LSCs (Table 7). However, σ declined significantly after the second firing, possibly as a result of altered lithium disilicate crystal sizes (Table 6) causing residual stresses within the surrounding glass matrix and thus interfering with crystal interlocking.[67] Deteriorating effects of repeated firing have been reported for dental ceramics[22,69] and are credited to diminished favorable compressive stresses introduced

Table 7. Characteristic strength σ_0 (MPa), Weibull modulus (*m*), and coefficient of determination (R^2) of computer-aided design and computer-aided manufacturing lithium silicate-based glass-ceramics after heat treatment by ball-on-3-ball method

Group	Characteristic Strength σ_0 (MPa)	Characteristic Strength σ_0 (MPa) [95% CI]	Weibull Modulus (m)	Weibull Modulus (m) [95% CI]	Coefficient of Determination (R^2)
LS - NF	632.7	[588.6-681.7]	8.9	[4.9-12.1]	0.899
LS – F1	651.9	[617.6-689.3]	11.9	[6.6-16.1]	0.858
LS – F2	478.2	[446.9-512.8]	9.5	[5.3-12.9]	0.943
LS – GF1	415.7	[393.5-439.9]	11.7	[6.5-15.9]	0.944
LS – GF2	327	[303.1-353.6]	8.5	[4.7-11.5]	0.966
CD – NF	713.4	[651.1-784.0]	7.2	[3.9-9.5]	0.888
CD – F1	812.4	[781.9-845.1]	16.8	[9.3-22.9]	0.961
CD – F2	658.5	[633.0-685.8]	16.3	[9.0-22.1]	0.876
CD – GF1	645.5	[592.8-704.8]	7.5	[4.2-10.2]	0.841
CD – GF2	411.6	[379.8-447.2]	8.0	[4.4-10.9]	0.951
CT – NF	327	[301.3-355.8]	7.8	[4.4-10.7]	0.974
CT – F1	502.7	[469.2-539.7]	9.4	[5.2-12.7]	0.929
CT – F2	473.4	[435.5-515.9]	7.7	[4.3-10.5]	0.958
CT – GF1	368.7	[333.3-409.2]	6.4	[3.5-8.6]	0.950
CT – GF2	317.3	[289.7-348.6]	7.0	[3.9-9.6]	0.943

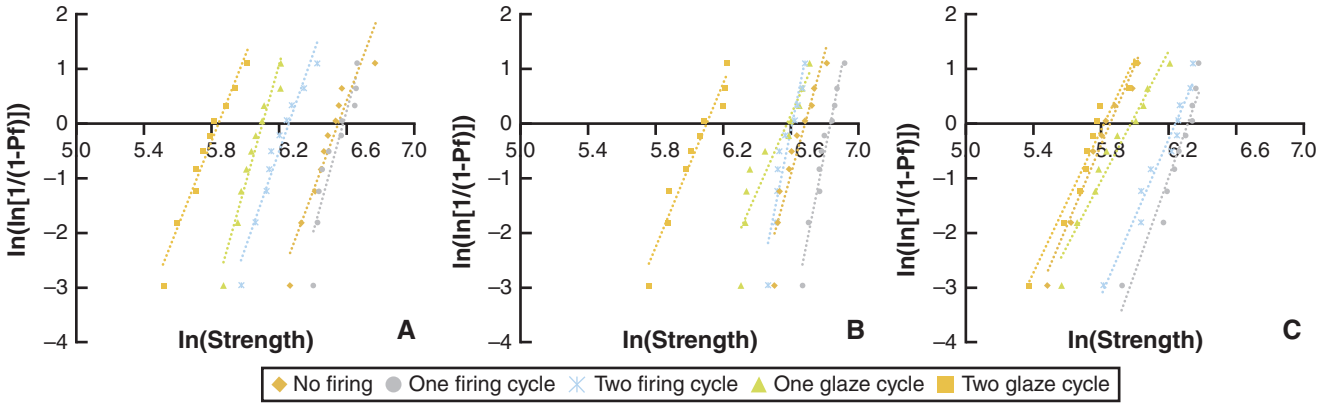

Figure 5. Weibull probability plots for lithium silicate-based glass-ceramics following different heat treatments. A, Initial LiSi blocks. B, Celtra Duo. C, CEREC Tessera.

during polishing.[69,70] A decrease in σ after extended sintering and glazing treatments has also been reported.[13,22,28,30,46] While glazing enhances surface texture, it can generate inherent interface stresses that initiate microcracks in the underlying ceramics.[28,30]

Weibull statistics are recommended for brittle materials when σ data accurately fit the plotted analysis model (R^2>0.84) (Fig. 5).[59] Ceramics with high Weibull modulus display improved homogeneity and reliability and less strength variability.[10] In the present study, σ_0 and m values fell within the previously reported range[49,71]; the highest reliability was displayed by CD after 1 firing cycle (m=16.8, whereas single glazed CT had the lowest reliability (m=6.4) (Table 7), suggesting a wide distribution of strength-limiting defects in the glazed CT materials. Repeated firing decreased LSC homogeneity as determined by reduced m values in the F2 treatment groups compared with those in F1. The glazing smoothening effect (Fig. 2A) has been predicted to improve σ by eliminating surface flaws,[28] yet strength results prove otherwise; glazing reduced the σ_0 of LD and CD (by 50%) to a greater extent than CT (30%) (Table 7). Glazing leads to residual stresses within ceramics because of the thermal expansion mismatch throughout firing and cooling[32,33]; however, this phenomenon should be investigated in studies through finite element analysis that assesses stress distributions and fractographic behaviors during dynamic loading.

Limitations of the present study included that all experiments were executed in a dry room-temperature environment on square plates, as they do not precisely simulate dental restorations in situ intraorally. Based on the findings of this study, fully crystallized LSC restorations should be exposed to 1 sintering cycle, as it limits machining-induced strength-limiting flaws. However, additional firing treatments may negatively impact LSC performance and should be approached with caution. Furthermore, if minor intraoral adjustments are performed on glazed LSC restorations that violate the glaze layer integrity, adequate polishing protocols should be performed instead of reglazing because of the favorable compressive stresses generated by polishing in contrast with the weakening tensile stresses that may stem from glazing.

CONCLUSIONS

Based on the findings of this in vitro study, the following conclusions were drawn:

1. Repeated firing treatments altered the surface topography and gloss of fully crystallized CAD-CAM LSCs within clinically acceptable values.
2. The attenuation of irradiance of a light-polymerizing unit was significantly influenced by the chemical composition of interposed fully crystallized CAD-CAM LSCs in combination with the presence of a glaze layer.
3. The Martens hardness of fully crystallized CAD-CAM LSCs was significantly reduced after the second firing cycle and after glazing cycles.
4. Limited changes in the crystalline microstructure of fully crystallized CAD-CAM LSCs were detected after the firing treatments.
5. Glazing fully crystallized CAD-CAM LSCs significantly reduced their biaxial flexural strength in comparison with unglazed ceramics.

REFERENCES

1. Lubauer J, Belli R, Peterlik H, Hurle K, Lohbauer U. Grasping the lithium hype: Insights into modern dental lithium silicate glass-ceramics. *Dent Mater*. 2022;38:318–332.
2. Marchesi G, Camurri Piloni A, Nicolin V, Turco G, Di Lenarda R. Chairside CAD/CAM materials: Current trends of clinical uses. *Biology*. 2021;10:1170.
3. Phark JH, Duarte Jr S. Microstructural considerations for novel lithium disilicate glass ceramics: A review. *J Esthet Restor Dent*. 2022;34:92–103.
4. Riquieri H, Monteiro JB, Viegas DC, Campos TMB, de Melo RM, Saavedra GdSFA. Impact of crystallization firing process on the microstructure and flexural strength of zirconia-reinforced lithium silicate glass-ceramics. *Dent Mater*. 2018;34:1483–1491.

5. Krüger S, Deubener J, Ritzberger C, Höland W. Nucleation kinetics of lithium metasilicate in ZrO2–bearing lithium disilicate glasses for dental application. *Int J Appl Glass Sci*. 2013;4:9–19.
6. Chen X-P, Xiang Z-X, Song X-F, Yin L. Machinability: Zirconia-reinforced lithium silicate glass ceramic versus lithium disilicate glass ceramic. *J Mech Behav Biomed Mater*. 2020;101:103435.
7. de Matos JDM, Lopes GRS, Queiroz DA, et al. Dental ceramics: Fabrication methods and aesthetic characterization. *Coatings*. 2022;12:1228.
8. Jurado CA, El-Gendy T, Hyer J, Tsujimoto A. Color stability of fully- and pre-crystalized chair-side CAD-CAM lithium disilicate restorations after required and additional sintering processes. *J Adv Prosthodont*. 2022;14:56–62.
9. Miranda JS, Barcellos AS, MartinelliLobo CM, Caneppele TM, Amaral M, Kimpara ET. Effect of staining and repeated firing on the surface and optical properties of lithium disilicate. *J Esthet Restor Dent*. 2020;32:113–118.
10. Schweitzer F, Spintzyk S, Geis-Gerstorfer J, Huettig F. Influence of minimal extended firing on dimensional, optical, and mechanical properties of crystalized zirconia-reinforced lithium silicate glass ceramic. *J Mech Behav Biomed Mater*. 2020;104:103644.
11. Reid D, Matis J, Lien W, et al. Optical and mechanical properties of new ceramic CAD/CAM materials. *Oper Dent*. 2023;48:425–434.
12. Jurado CA, Afrashtehfar KI, Hyer J, Alhotan A. Effect of sintering on the translucency of CAD–CAM lithium disilicate restorations: A comparative in vitro study. *J Prosthodont*. 2023;3:861–866.
13. Lu Y, Dal Piva AMO, Nedeljkovic I, Tribst JPM, Feilzer AJ, Kleverlaan CJ. Effect of glazing technique and firing on surface roughness and flexural strength of an advanced lithium disilicate. *Clin Oral Investig*. 2023;27:3917–3926.
14. Lawson NC, Bansal R, Burgess JO. Wear, strength, modulus and hardness of CAD/CAM restorative materials. *Dent Mater*. 2016;32:e275–e283.
15. Diniz V, Condé Oliveira Prado PH, Meireles Rodrigues JV, et al. Ceramic firing protocols and thermocycling: Effects on the load-bearing capacity under fatigue of a bonded zirconia lithium silicate glass-ceramic. *J Mech Behav Biomed Mater*. 2020;110:103963.
16. Badawy R, El-Mowafy O, Tam LE. Fracture toughness of chairside CAD/CAM materials – Alternative loading approach for compact tension test. *Dent Mater*. 2016;32:847–852.
17. Diniz V, Monteiro JB, Rodrigues JVM, Prado P, Melo RM. Impact of acid concentration and firing on the long-term bond strength of a zirconia-lithium silicate ceramic following adhesive cementation. *J Adhes Dent*. 2019;21:355–363.
18. Rodrigues MR, Grangeiro MTV, Rossi NR, et al. Influence of optional crystallization firing on the adhesion of zirconia-reinforced lithium silicate before and after aging. *Coatings*. 2022;12:1904.
19. Moeeduddin M, Nathanson D, Fan Y. Effect of firing cycle and etching protocols on tensile bond strength of composite cement to zirconium-incorporated lithium-silicate glass ceramic. *J Adhes Dent*. 2020;22:625–633.
20. Itthipongsatorn N, Srisawasdi S. Dentin microshear bond strength of various resin luting agents to zirconia-reinforced lithium silicate ceramics. *J Prosthet Dent*. 2020;124:237.e1–237.e7.
21. Zaniboni JF, Silva AM, Alencar CdM, et al. Influence of different glaze firing protocols on the mechanical properties of CAD-CAM ceramic materials. *J Prosthet Dent*. 2022;127:925.e1–925.e8.
22. Aurélio IL, Fraga S, Dorneles LS, Bottino MA, May LG. Extended glaze firing improves flexural strength of a glass ceramic. *Dent Mater*. 2015;31:e316–e324.
23. Aksoy G, Polat H, Polat M, Coskun G. Effect of various treatment and glazing (coating) techniques on the roughness and wettability of ceramic dental restorative surfaces. *Colloid Surf B: Biointerfaces*. 2006;53:254–259.
24. Kurt M, Bankoğlu Güngör M, Karakoca Nemli S, Turhan Bal B. Effects of glazing methods on the optical and surface properties of silicate ceramics. *J Prosthodont Res*. 2020;64:202–209.
25. Klein C, Krespach M, Spintzyk S, Wolff D, von Ohle C, Meller C. Restorative CAD/CAM materials in dentistry: Analysis of their fluorescence properties and the applicability of the fluorescence-aided identification technique (FIT). *Clin Oral Investig*. 2021;25:4579–4589.
26. Revilla-León M, Sorensen JA, Nelson LY, Gamborena I, Yeh YM, Özcan M. Effect of fluorescent and nonfluorescent glaze pastes on lithium disilicate pressed ceramic color at different thicknesses. *J Prosthet Dent*. 2021;125:932–939.
27. Volpato CAM, Pereira MRC, Silva FS. Fluorescence of natural teeth and restorative materials, methods for analysis and quantification: A literature review. *J Esthet Restor Dent*. 2018;30:397–407.
28. Fairhurst C, Lockwood P, Ringle R, Thompson W. The effect of glaze on porcelain strength. *Dent Mater*. 1992;8:203–207.
29. Baharav H, Laufer B-Z, Pilo R, Cardash HS. Effect of glaze thickness on the fracture toughness and hardness of alumina-reinforced porcelain. *J Prosthet Dent*. 1999;81:515–519.
30. Albakry M, Guazzato M, Swain MV. Effect of sandblasting, grinding, polishing and glazing on the flexural strength of two pressable all-ceramic dental materials. *J Dent*. 2004;32:91–99.
31. Inokoshi M, Zhang F, Vanmeensel K, et al. Residual compressive surface stress increases the bending strength of dental zirconia. *Dent Mater*. 2017;33:e147–e154.
32. Kumchai H, Juntavee P, Sun AF, Nathanson D. Effect of glazing on flexural strength of full-contour zirconia. *Int J Dent*. 2018;2018.
33. Deville S, Chevalier J, Gremillard L. Influence of surface finish and residual stresses on the ageing sensitivity of biomedical grade zirconia. *Biomater*. 2006;27:2186–2192.
34. Jones C, Billington R, Pearson G. The in vivo perception of roughness of restorations. *Br Dent J*. 2004;196:42–45.
35. Bollen CM, Papaioanno W, Van Eldere J, Schepers E, Quirynen M, Van Steenberghe D. The influence of abutment surface roughness on plaque accumulation and peri-implant mucositis. *Clin Oral Implants Res*. 1996;7:201–211.
36. Lawson NC, Janyavula S, Syklawer S, McLaren EA, Burgess JO. Wear of enamel opposing zirconia and lithium disilicate after adjustment, polishing and glazing. *J Dent*. 2014;42:1586–1591.
37. da Costa JB, Ferracane JL, Amaya-Pajares S, Pfefferkorn F. Visually acceptable gloss threshold for resin composite and polishing systems. *J Am Dent Assoc*. 2021;152:385–392.
38. Shen C, Rawls HR, Esquivel-Upshaw JF. Phillips' Science of Dental Materials. 13th ed.,. Elsevier Health Sciences,; 2021:87–114.
39. Carrabba M, Vichi A, Vultaggio G, Pallari S, Paravina R, Ferrari M. Effect of finishing and polishing on the surface roughness and gloss of feldspathic ceramic for chairside CAD/CAM systems. *Oper Dent*. 2017;42:175–184.
40. Broitman E. Indentation hardness measurements at macro-, micro-, and nanoscale: A critical overview. *Tribol Lett*. 2017;65:23.
41. Shahdad SA, McCabe JF, Bull S, Rusby S, Wassell RW. Hardness measured with traditional Vickers and Martens hardness methods. *Dent Mater*. 2007;23:1079–1085.
42. Hampe R, Lümkemann N, Sener B, Stawarczyk B. The effect of artificial aging on Martens hardness and indentation modulus of different dental CAD/CAM restorative materials. *J Mech Behav Biomed Mater*. 2018;86:191–198.
43. Mörmann WH, Stawarczyk B, Ender A, Sener B, Attin T, Mehl A. Wear characteristics of current aesthetic dental restorative CAD/CAM materials: Two-body wear, gloss retention, roughness and Martens hardness. *J Mech Behav Biomed Mater*. 2013;20:113–125.
44. Stawarczyk B, Awad D, Ilie N. Blue-light transmittance of esthetic monolithic CAD/CAM materials with respect to their composition, thickness, and curing conditions. *Oper Dent*. 2016;41:531–540.
45. Romanyk DL, Guo Y, Rae N, et al. Strength-limiting damage and its mitigation in CAD-CAM zirconia-reinforced lithium-silicate ceramics machined in a fully crystallized state. *Dent Mater*. 2020;36:1557–1565.
46. Li D, Guo J, Wang X, Zhang S, He L. Effects of crystal size on the mechanical properties of a lithium disilicate glass-ceramic. *Mater Sci Eng*. 2016;669:332–339.
47. Börger A, Supancic P, Danzer R. The ball on three balls test for strength testing of brittle discs: Stress distribution in the disc. *J Eur Ceram Soc*. 2002;22:1425–1436.
48. Rasche S, Strobl S, Kuna M, Bermejo R, Lube T. Determination of strength and fracture toughness of small ceramic discs using the small punch test and the ball-on-three-balls test. *Proc Mater Sci*. 2014;3:961–966.
49. Wendler M, Belli R, Petschelt A, et al. Chairside CAD/CAM materials. Part 2: Flexural strength testing. *Dent Mater*. 2017;33:99–109.
50. Danzer R, Harrer W, Supancic P, Lube T, Wang Z, Börger A. The ball on three balls test—Strength and failure analysis of different materials. *J Eur Ceram Soc*. 2007;27:1481–1485.
51. Garoushi S, Säilynoja E, Vallittu PK, Lassila L. Fracture-behavior of CAD/CAM ceramic crowns before and after cyclic fatigue aging. *Int J Prosthodont*. 2023;36:649.
52. Stawarczyk B, Özcan M, Trottmann A, Schmutz F, Roos M, Hämmerle C. Two-body wear rate of CAD/CAM resin blocks and their enamel antagonists. *J Prosthet Dent*. 2013;109:325–332.
53. ISO 25178–1:2017 - Surface texture: Areal - Part 71: Software measurement standards 2017. International Organization for Standardization 2017.
54. EN ISO 2813. Paints and varnishes-Determination of gloss value at 20 degrees, 60 degrees and 85 degrees. International Organization for Standardization 2014.
55. Mayinger F, Lümkemann N, Musik M, Eichberger M, Stawarczyk B. Comparison of mechanical properties of different reinforced glass-ceramics. *J Prosthet Dent*. 2022;127:146–153.
56. BS EN ISO 14577–4:2016. Metallic materials — instrumented indentation test for hardness and materials parameters — Part 4: test method for metallic and non-metallic coatings. International Organization for Standardization 2016.
57. Supornpun N, Oster M, Phasuk K, Chu T-MG. Effects of shade and thickness on the translucency parameter of anatomic-contour zirconia, transmitted light intensity, and degree of conversion of the resin cement. *J Prosthet Dent*. 2023;129:213–219.
58. Patterson AL. The Scherrer formula for X-ray particle size determination. *Phys Rev*. 1939;56:978–982.

59. Quinn JB, Quinn GD. A practical and systematic review of Weibull statistics for reporting strengths of dental materials. *Dent Mater.* 2010;26:135–147.
60. 843–5 DE. Advanced technical ceramics-Monolithic ceramics; mechanical tests at room temperature-Part 5: statistical analysis. Dtsch Inst Fur Norm–DIN. 2007.
61. Lakens D. Calculating and reporting effect sizes to facilitate cumulative science: A practical primer for t-tests and ANOVAs. *Front Psychol.* 2013;4:863.
62. Dentistry - Ceramic Materials BS EN ISO 6872:2015+A1:2018. International Organization for Standardization 2018.
63. Gonuldas F, Yılmaz K, Ozturk C. The effect of repeated firings on the color change and surface roughness of dental ceramics. *J Adv Prosthodont.* 2014;6:309–316.
64. Özdemir H, Özdoğan A. The effect of heat treatments applied to superstructure porcelain on the mechanical properties and microstructure of lithium disilicate glass ceramics. *Dent Mater J.* 2018;37:24–32.
65. Sarıkaya I, Hayran Y. Effects of polishing on color stability and surface roughness of CAD-CAM ceramics. *Meandros Med Dent J.* 2018;19:153.
66. Akar GC, Pekkan G, Çal E, Eskitaşçıoğlu G, Özcan M. Effects of surface-finishing protocols on the roughness, color change, and translucency of different ceramic systems. *J Prosthet Dent.* 2014;112:314–321.
67. Ozdogan A, Ozdemir H. Effects of multiple firing processes on the mechanical properties of lithium disilicate glass-ceramics produced by two different production techniques. *J Prosthet Dent.* 2021;125.
68. Tang X, Nakamura T, Usami H, Wakabayashi K, Yatani H. Effects of multiple firings on the mechanical properties and microstructure of veneering ceramics for zirconia frameworks. *J Dent.* 2012;40:372–380.
69. Gozneli R, Kazazoglu E, Ozkan Y. Flexural properties of leucite and lithium disilicate ceramic materials after repeated firings. *J Dent Sci.* 2014;9:144–150.
70. Giordano R, Cima M, Pober R. Effect of surface finish on the flexural strength of feldspathic and aluminous dental ceramics. *Int J Prosthodont.* 1995;8:311–319.
71. Lima CM, da Silva NR, Martins JD, et al. Effect of different surface treatments on the biaxial flexure strength, Weibull characteristics, roughness, and surface topography of bonded CAD/CAM silica-based ceramics. *Dent Mater.* 2021;37:e151–e161.

Corresponding author:
Professor Nick Silikas
Division of Dentistry
School of Medical Sciences
University of Manchester
Coupland 3 Building
Oxford Road
Manchester, England M13 9PL
UK
Email: nikolaos.silikas@manchester.ac.uk

Acknowledgments
The authors thank Dr Gary Miller in the Faculty of Science and Engineering at Manchester Metropolitan University (Manchester, England) for their contributions with their experimental work on the X-ray diffraction analysis.

CRediT authorship contribution statement
Hanan Al-Johani: Conceptualization, Methodology, Software, Data curation, Investigation, Formal analysis, Writing- original draft preparation. **Julfikar Haider:** Software, Validation, Visualization, Writing- reviewing and editing. **Nick Silikas:** Conceptualization,Writing- reviewing and editing. **Julian Satterthwaite:** Conceptualization,Writing- reviewing and editing.

https://doi.org/10.1016/j.prosdent.2024.01.006